

Hollow Hematite Spheres and their Applications in Gas Sensors and Li-ion Batteries

Hyo-Joong Kim,^a Kwon-Il Choi,^a Anqiang Pan,^{bc} Il-Doo Kim,^d Hae-Ryong Kim,^a Kang-Min Kim,^a Chan Woong Na,^a Guozhong Cao,^{*b}, and Jong-Heun Lee^{*a}

^aDepartment of Materials Science and Engineering, Korea University, Seoul 136-713, Republic of Korea

^bDepartment of Materials Science and Engineering, University of Washington, Seattle, Washington 98195, USA

^cDepartment of Materials Science and Engineering, Central South University, Hunan, 410083, China

^dOptoelectronic Materials Center, Korea Institute of Science and Technology, Seoul 130-650, Republic of Korea

*To whom correspondence should be addressed.

Phone: +82-3290-3282, Fax: +82-2-928-3584, email: jongheun@korea.ac.kr

Phone: +1-206-616-9084, Fax: +1-206-543-2101, email: gzcao@u.washington.edu

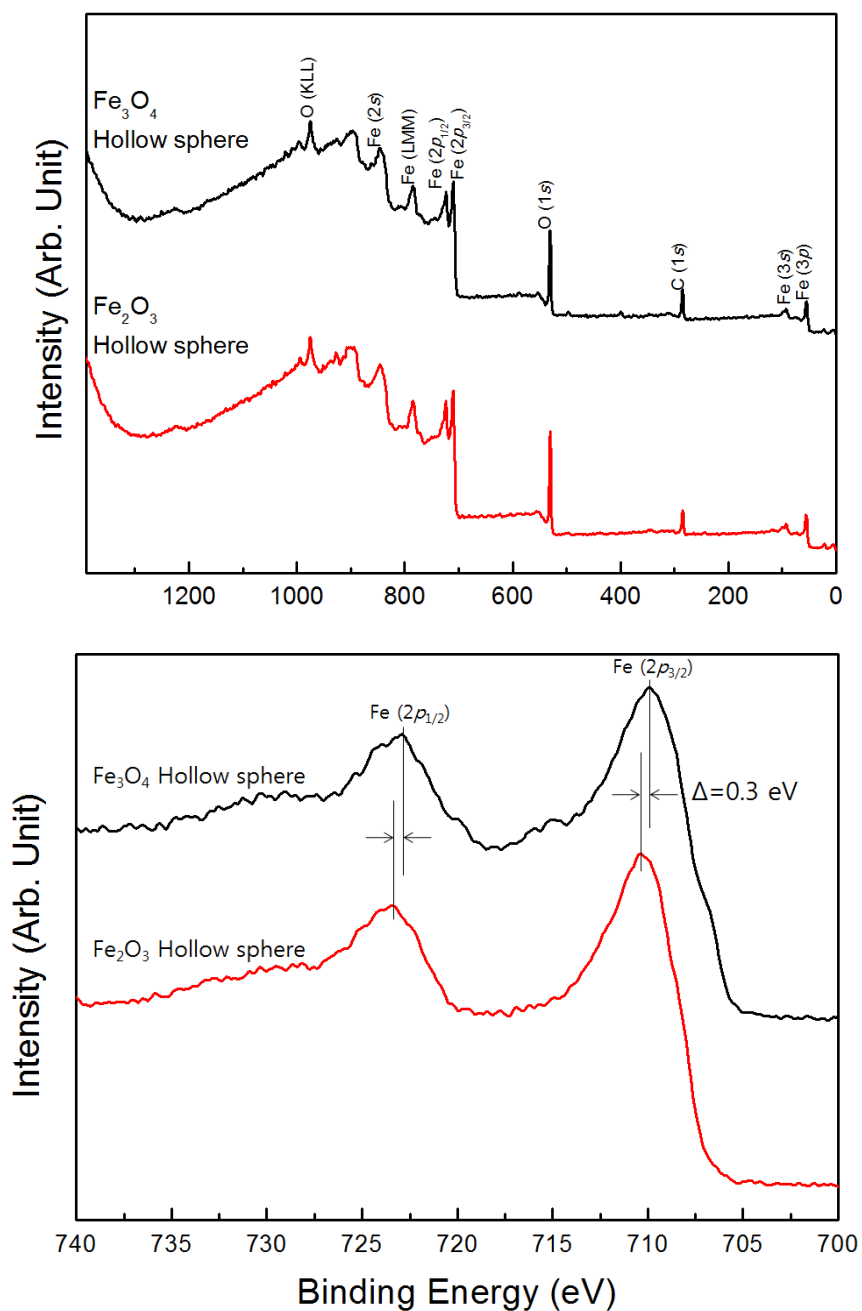


Fig. S1 X-ray photoelectron spectroscopy results of as-prepared Fe₃O₄ hollow spheres and Fe₂O₃ hollow spheres after heat treatment at 500°C for 2 h. The binding energies for Fe 2p_{1/2} and Fe 2p_{3/2} peaks of as-prepared Fe₃O₄ hollow spheres were ~ 0.3 eV lower than those of heat-treated Fe₂O₃ hollow spheres. This indicates that the as-prepared specimens contain Fe²⁺ and can be identified as Fe₃O₄ rather than γ -Fe₂O₃.

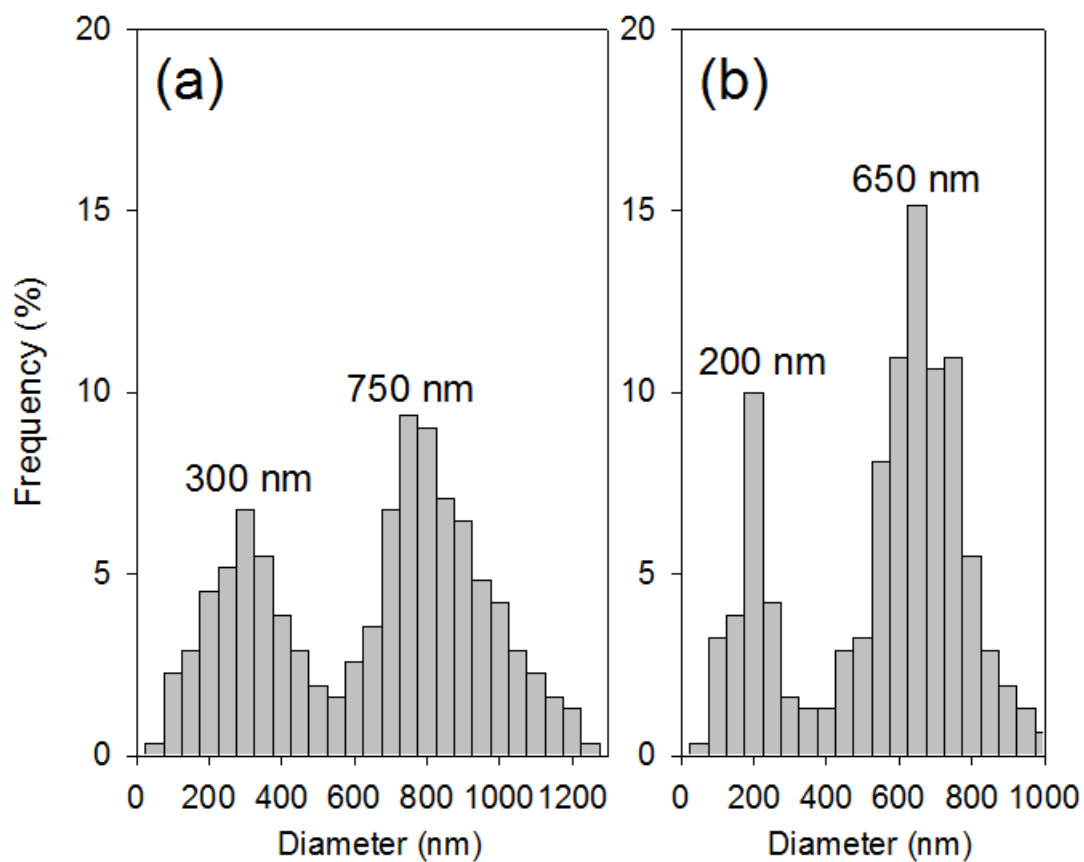


Fig. S2 Particle size distribution of (a) as-prepared Fe₃O₄ hollow spheres and (b) Fe₂O₃ hollow spheres after heat treatment at 500°C for 2 h. The diameters of 310 particles were measured for each specimen to get the particle size distribution. The two sizes in each graph are the mode diameters of bimodal particle size distribution.

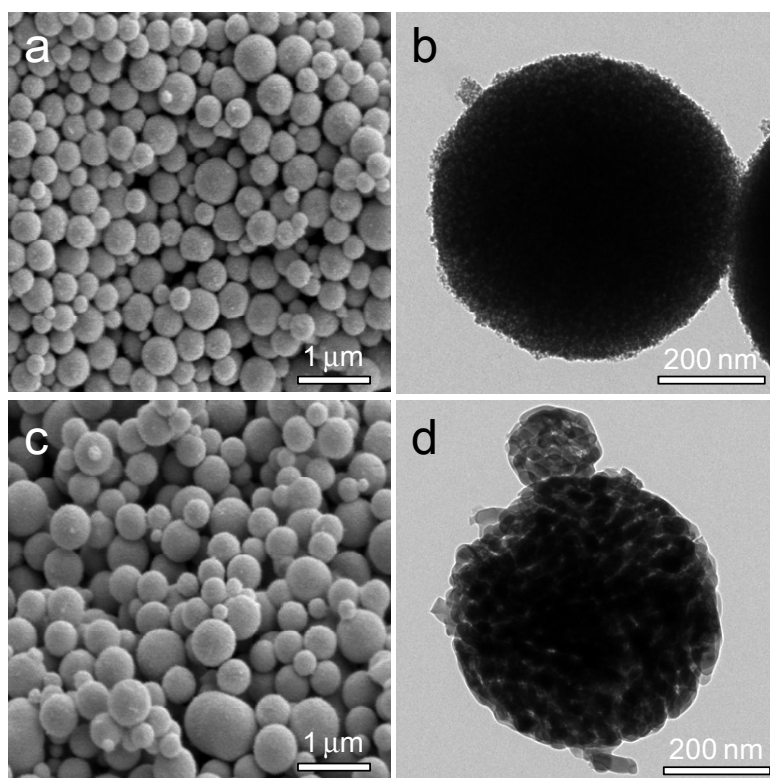
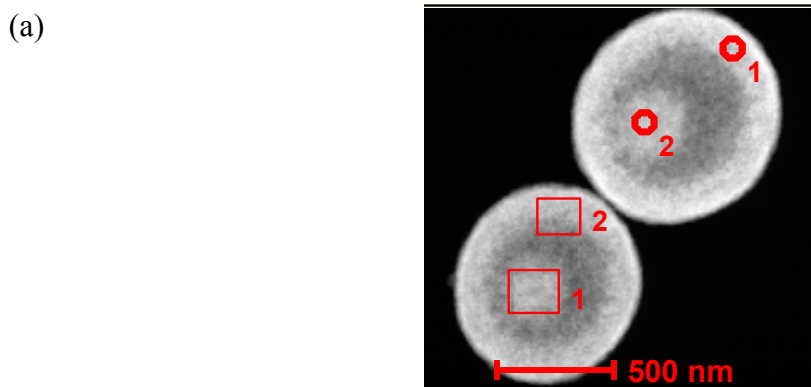
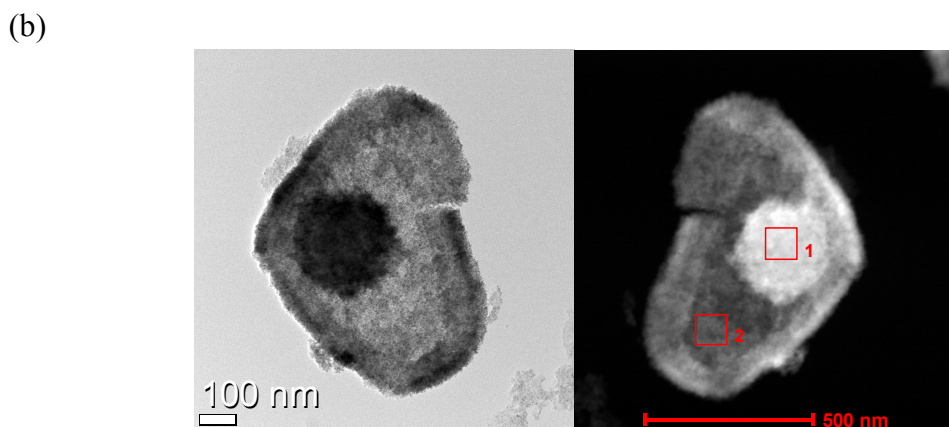


Fig. S3 SEM and TEM images of (a), (b) as-prepared Fe_3O_4 and (c), (d) Fe_2O_3 solid spheres after heat treatment at 500°C for 2 h. The spheres with solid inner structures were prepared by the solvothermal reaction of $\text{C}_2\text{H}_5\text{OH}$ solution containing only $\text{Fe}(\text{CH}_3\text{CHOO})_2$.



	Outer Point (O1)	Inner point (O2)	Outer area (2)	Inner area (1)
C	58.15	71.32	52.91	63.53
N	5.77	8.65	8.24	9.63
O	22.59	13.74	24.38	18.64
Fe	11.73	6.27	14.44	8.18

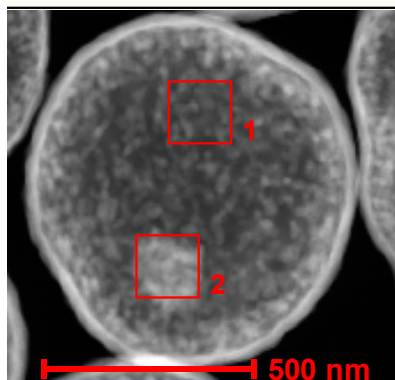
(atomic %)



	Area 1	Area 2
C	78.71	71.03
N	6.13	2.52
O	9.31	13.63
Fe	5.85	12.82

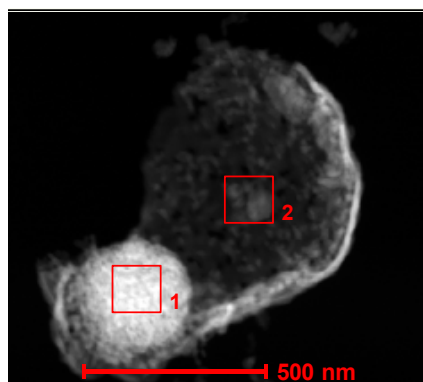
(atomic %)

Fig. S4 EDS analysis results of as-prepared hollow spheres: (a) hollow spheres and (b) broken hollow spheres.



	Area 1	Area 2
C	22.77	11.76
O	48.92	56.67
Fe	28.30	31.55

(atomic %)



	Area 1	Area 2
C	21.92	61.56
O	44.03	25.42
Fe	34.05	13.02

(atomic %)

Fig. S5 EDS analysis results of Fe_2O_3 hollow spheres after heat treatment at 500°C for 2 h: (a) hollow spheres and (b) broken hollow spheres.

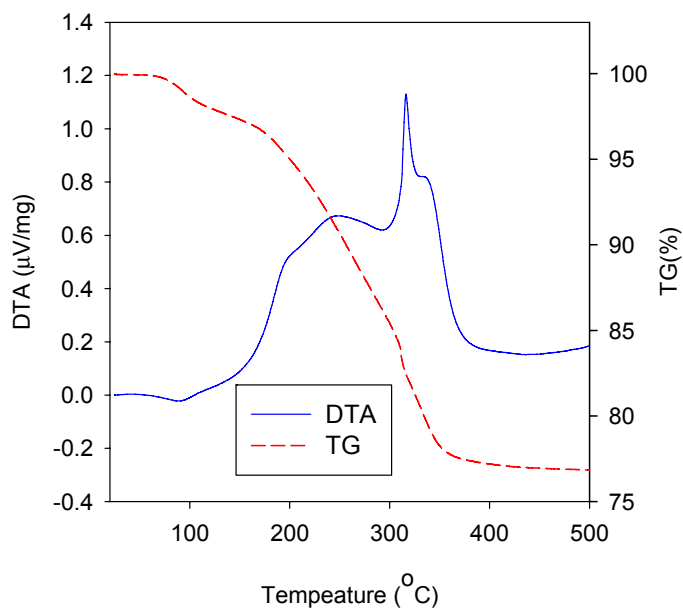


Fig. S6 DTA and TG curves of as-prepared Fe_3O_4 hollow spheres.

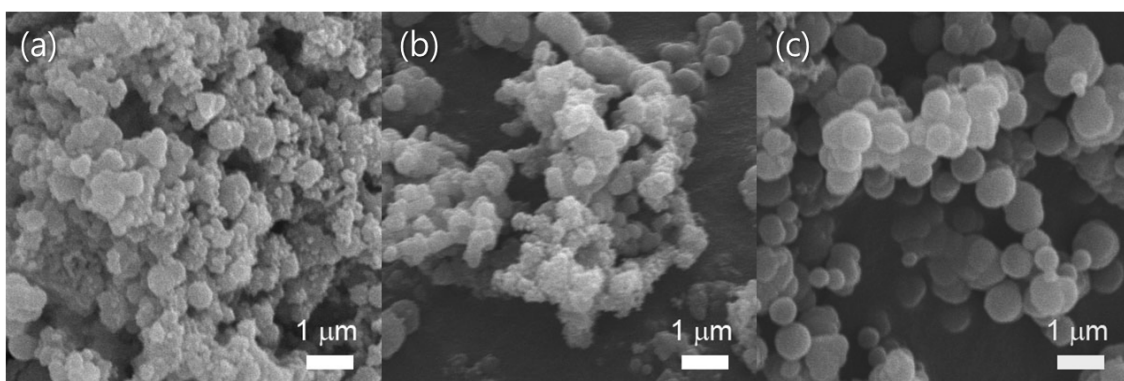


Fig. S7 Morphologies of the products after solvothermal reaction of ethanol solution containing iron (II) acetate and L(+)-Lysine at 200 °C (a) for 0.5 h, (b) 1 h and (c) 2 h.

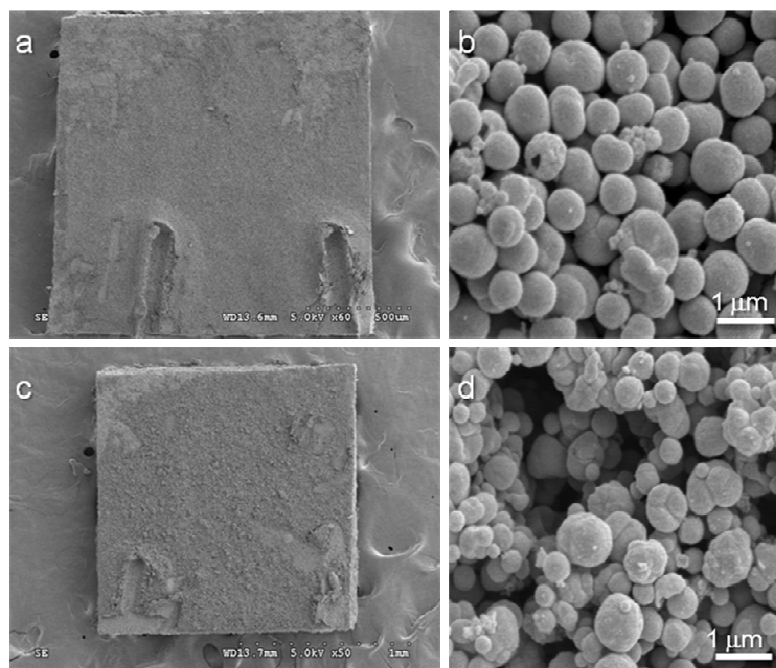
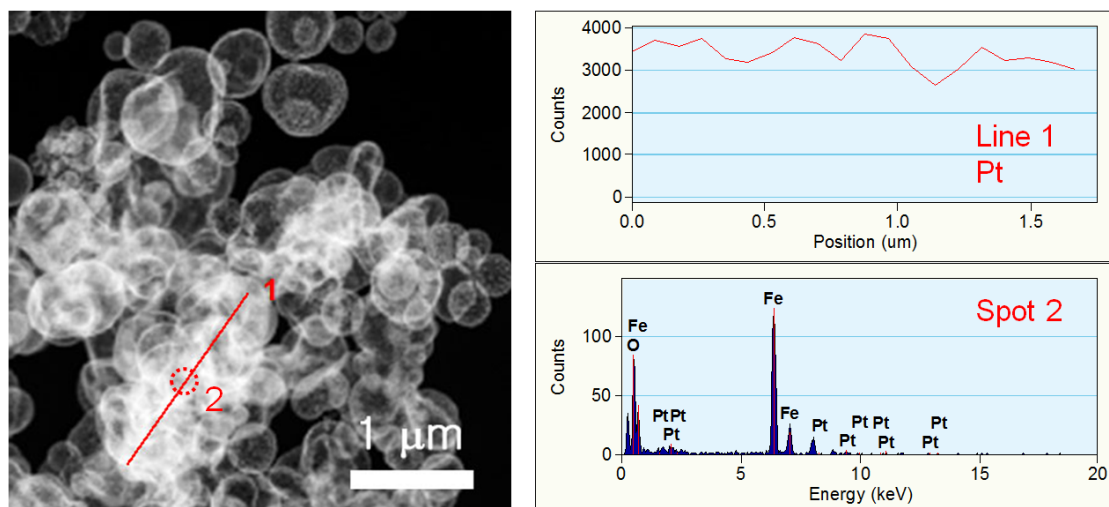


Fig. S8 The low and high magnification images of sensor surfaces: (a,b) Fe_2O_3 hollow spheres sensor; and (c,d) Pt-doped Fe_2O_3 hollow spheres sensor.



Spot 1	
O (K)	53.34
Fe (K)	45.45
Pt (L)	1.21

(atomic %)

Fig. S9 EDS analysis results of Pt-doped Fe₂O₃ hollow spheres after heat treatment at 500°C for 2 h.

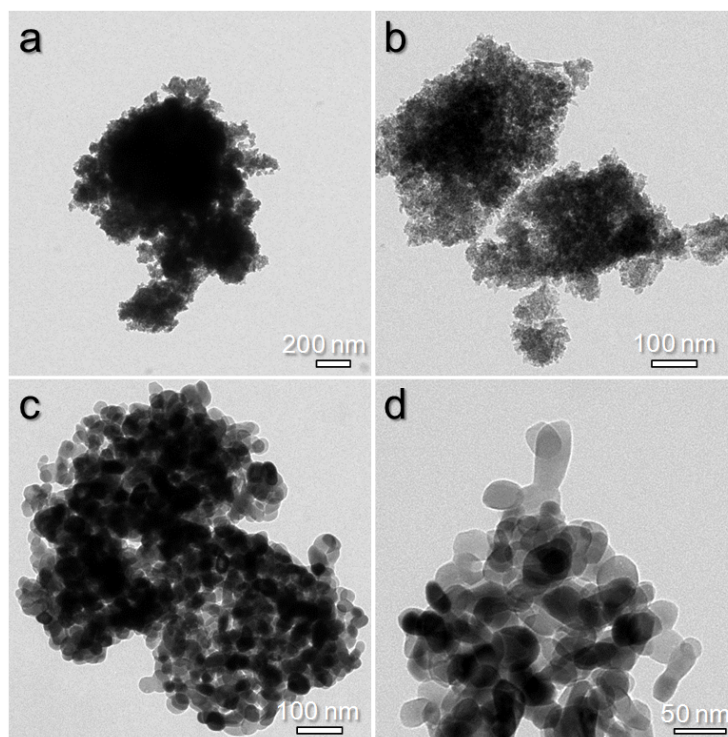


Fig. S10 TEM images of (a,b) Fe-precursors prepared by carbonate precipitation and (c,d) Fe_2O_3 agglomerated nanoparticles after heat treatment at 500°C for 2 h.

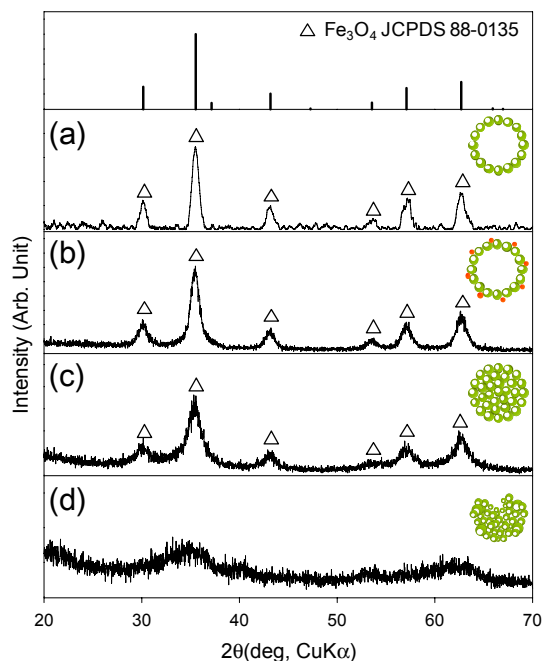


Fig. S11 X-ray diffraction patterns of (a) as-prepared Fe_3O_4 hollow spheres, (b) as-prepared Pt-doped Fe_3O_4 hollow spheres, (c) as-prepared Fe_3O_4 solid spheres, and (d) as-prepared Fe-carbonate precursors.

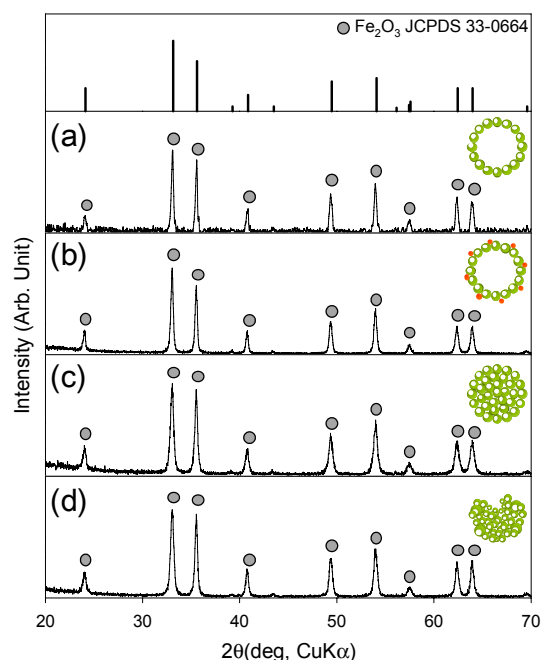


Fig. S12 X-ray diffraction patterns of (a) Fe_2O_3 hollow spheres, (b) Pt-doped Fe_2O_3 hollow spheres, (c) Fe_2O_3 solid spheres, and (d) Fe_2O_3 agglomerated nanoparticles after heat treatment at 500°C for 2 h.

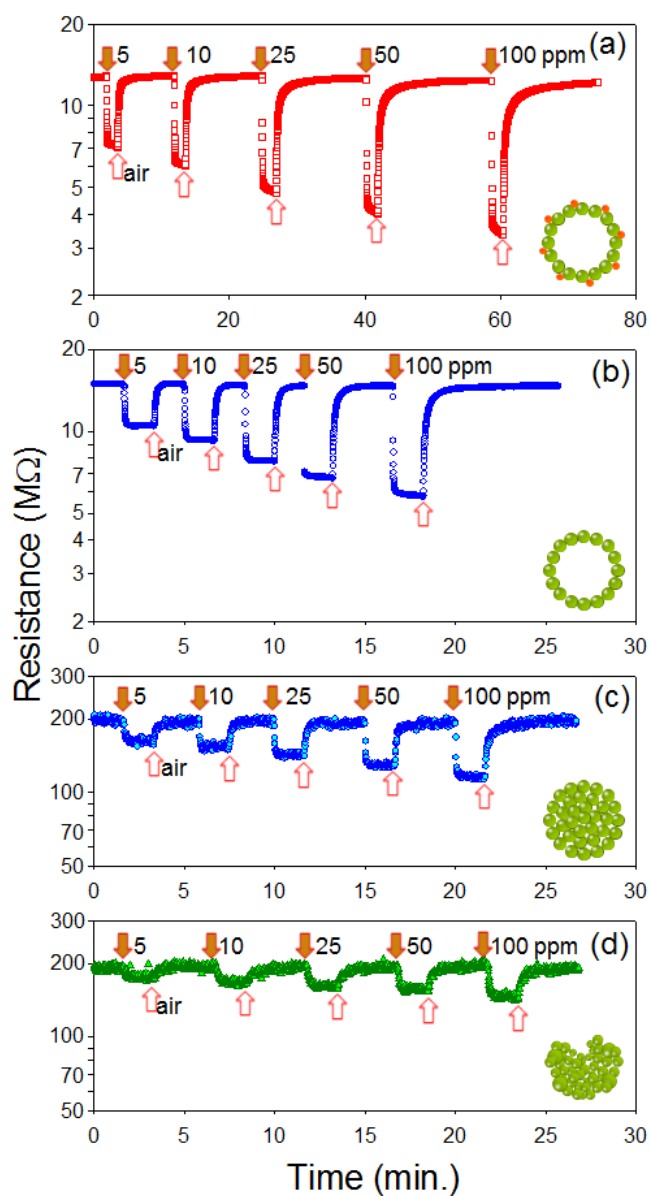


Fig. S13 Ethanol sensing transients of (a) Pt-doped Fe_2O_3 hollow spheres, (b) Fe_2O_3 hollow spheres, (c) Fe_2O_3 solid spheres, and (d) Fe_2O_3 agglomerated nanoparticles at the sensing temperature of $400^\circ C$.